Journal of Metals, Materials and Minerals, Vol. 31, No. 4, pp. 143-150, 2021

Influence of graphite feedstock on the characteristics of silver-decorated graphene oxide and antimicrobial property

Ebrahim MAHMOUDI[1], Wei Lun ANG[1,*], Gasidit PANOMSUWAN[2], Oratai JONGPRATEEP[2], Abdul Wahab MOHAMMAD[1], Law Yong NG[3], and Muneer M. BA-ABBAD[4]

[1] *Department of Chemical and Process Engineering, Faculty of Engineering and Built Environment, Universiti Kebangsaan Malaysia, 43600 Bangi, Selangor, Malaysia*

[2] *Department of Materials Engineering, Faculty of Engineering, Kasetsart University, Bangkok 10900, Thailand*

[3] *Department of Chemical Engineering, Lee Kong Chian Faculty of Engineering and Science, Universiti Tunku Abdul Rahman, Jalan Sungai Long, Bandar Sungai Long, Cheras, 43000 Kajang, Selangor, Malaysia*

[4] *Gas Processing Centre, Qatar University, P.O. Box 2713, Doha, Qatar*

***Corresponding author e-mail:** wl_ang@ukm.edu.my

Received date:
16 August 2021
Revised date
12 October 2021
Accepted date:
28 October 2021

Keywords:
Graphite sources;
Silver-graphene oxide composite;
Antimicrobial;
Nanoparticles

Abstract

Graphite from different sources has significant influence on the properties of graphene oxide (GO) and reactivity of GO towards further modification with other nanoparticles. However, such effect has not yet been properly explored. This study aims to investigate the characteristics and antimicrobial property of GO decorated with silver nanoparticles (known as Ag-GO composite) where the GO is synthesized via modified Hummer's method from various graphite feedstock, namely natural graphite flake (NGF), natural graphite powder (NGP), and synthetic graphite powder (SGP). The Ag-GO nanocomposite was then synthesized using chemical reduction methods. Antimicrobial properties of the Ag-GO were tested using the standard Kirby–Bauer antibiotic testing method with *E. coli* bacteria. Results showed that Ag-GO made from NGP has a smaller size and Ag nanoparticles (2 nm to 4 nm) were better distributed, and possessed better antimicrobial property. This phenomenon can be attributed to the higher number of functional groups on GO-NGP that can act as anchor sites for the nucleation of smaller-sized and well-dispersed Ag nanoparticles. It shows the significance of choosing the right graphite source where researchers can utilize to control the extent of decoration or coating of other nanoparticles on the synthesized GO to obtain the characteristics desired.

1. Introduction

Graphene oxide (GO) is a single atomic-layered carbon material in honeycomb lattice arrangement and laden with abundant reactive oxygen functional groups such as carboxyl, hydroxyl, and epoxy groups [1]. These functional groups of GO are responsible for its versatility and great acceptance in various material studies since the functional groups could be used as anchor points for the nucleation of nanoparticles such as silver and stabilizing them after their growth [2]. GO could be produced by oxidation and exfoliation of graphite, where the quality and characteristics of graphite sources will affect the properties of GO produced. Graphite with more defects will provide more active sites for oxidation, which subsequently offer more uniform distribution of nanomaterial decorated on the surface of GO due to the existence of numerous anchor points for nucleation growth of other materials [3].

In our previous work, we have studied the effect of different graphite sources, namely natural graphite flake (NGF), natural graphite powder (NGP), and synthetic graphite powder (SGP), on the properties of GO produced under the same reaction conditions [4,5]. It was discovered that the localized defects in the π–π structure of graphite could serve as a seed point for the oxidation of graphite to GO [6,7]. The higher the number of defects in π-π structure, the higher the degree of oxidation, thus indicating the presence of higher number of oxygen functional groups on GO. The abundance of functional groups of GO serve as good anchor points for functionalization where the nucleation, growth, and stabilization of metal and non-metal nanoparticles on GO could be conducted and promoted [3]. Functionalized GO is suitable for applications as high-performance nanocomposites, where a relatively small amount of fillers can be used to provide good mechanical properties. Hence, the functionalization of GO with different metallic and non-metallic nanoparticles such as GO-SnO_2, GO-TiO_2, GO-Co_3O_4, GO-mesoporous SiO_2, GO-Fe_3O_4, GO-Ag, and many more have been the subject of study for researchers [7-11]. Furthermore, GO has been functionalized using organic materials, dendrimers, and many types of nanopolymers [12-15]. Applying small-size nanoparticles has many challenges, including aggregation/agglomeration [16], which can lead to a reduction of mechanical properties [17] and leachate of nanoparticles into the surrounding environment [18]. Simultaneously, the aggregation/agglomeration phenomenon can adversely affect other properties, such as antimicrobial [19], surface charge, and thermal/

electrical conductivity [20], which render the functionalization of GO with nanoparticles less effective.

The stabilization and dispersion of nanomaterials have a direct effect on their properties and functionality. Many studies have focused on controlling the stability and dispersion of nanomaterials with the aim to change and/or enhance their properties [21]. The functionalization of GO with different nanomaterials is one of the methods employed by researchers to control the stability and dispersion of such nanomaterials [15]. As mentioned earlier, the oxygen functional groups of GO are anchor points for the nucleation of nanoparticles. Hence, GO with a higher number of functional groups could be an ideal material for the functionalization of nanomaterials, as well as to stabilize and uniformly disperse the nanomaterials. Silver (Ag) nanoparticles are an excellent example of size and dispersion dependency of nanomaterials [22]. Silver-based material has been used by ancient civilizations, specifically in agriculture and medical fields as antibacterial, antifungal, and antioxidants [19,23]. Hence many researchers studied the effect of Ag-nanoparticle size on antimicrobial effect, duration of sustained release of antibacterial, hydrophilicity of the Ag nanoparticles.

Silver decorated graphene oxide can serve as one of the innovative nanomaterials in the current research trend. There are a number of approaches used to synthesize silver decorated graphene oxide, such as chemical deposition [24], hydroquinone and silver nitrate reaction [25], reduction of silver nitrate using sodium hydroxide and phenolate anions [26], aqueous solution method using sodium borohydride method [27], in situ green synthesis [28], and green method using visible light [29]. The silver decorated graphene oxide showed higher antimicrobial properties in comparison to both graphene oxide and silver nanoparticles due to the synergistic effect of silver and graphene oxide and the size control that was achieved through the decoration of silver on graphene oxide [30]. For instance, Ag/GO composite exhibited strong antibacterial activity against *E. coli* by bringing the count of bacteria from 10^6 cfu·m^{-1} to zero in water [25]. The composite of Ag/GO also showed good potential in biomedical field, where the coating of Ag/GO on nickel-titanium alloy displayed antibacterial and antibiofilm effects on *Streptococcus mutans* biofilm [10,11].

In this work, the functionalization of Ag on GO produced from different graphite sources will be studied. This will verify the hypothesis that the graphite source with more defects will produce GO with a higher number of reactive functional groups, which is beneficial for the nucleation of Ag nanoparticles, and subsequently promoting the formation of more stable bonding between Ag and GO with uniform distribution. The hypothesis will be validated by looking at the dispersion of Ag on GO as well as its antibacterial property.

2. Experimental

2.1 Synthesis methodology

The synthesis of GO from different graphite sources using modified Hummers' method (NGF, NGP, and SGP) can be referred to in our previous publication [5,31]. The silver-decorated GO nanoplates were prepared by reducing silver nitrate ($AgNO_3$) with sodium borohydride ($NaBH_4$) in an aqueous GO solution [27]. During the preparation, 1 g of GO was added into 1 L of $AgNO_3$ aqueous solution (4×10^{-3} mol·dm^{-3}). A homogeneous suspension of GO can be obtained by sonication. The aqueous mixture was allowed to react while being continuously stirred for 1 h in an ice bath before the addition of a reducing agent. $NaBH_4$ solution (19 mL, 0.2 mol·dm^{-3}) was added slowly to the $AgNO_3$–GO suspension under vigorous stirring while the temperature was kept below 5°C. The colour of the mixture will turn grey. The reaction mixture was continuously stirred overnight at room temperature to ensure that the silver nitrate was completely reduced. Similar procedures were repeated with GO produced from different graphite sources. Silver decorated samples will be referred to as Ag-NGF, Ag-NGP, and Ag-SGP.

$$2\,AgNO_3 + 2\,NaBH_4 \rightarrow 2\,Ag_{(s)} + B_2H_{6\,(g)} + H_{2(g)} + 2\,NaNO_{3(s)} \quad (1)$$

2.2 Characterization of nanomaterials

The X-ray diffraction pattern of the self-synthesized silver oxide nanoparticles was measured using Bruker D8 Advance, Germany. Fourier Transform Infrared (FTIR) was carried out using a Nicolet 6700 Thermo Scientific- FITR spectrometer (United States). Transmission Electron Microscope (TEM) (CM 12 Philips model, The Netherlands) was used to visualize and measure the size of the silver nanoparticles decorated on GO. The light absorbance of the GO samples was determined using UV–visible spectrophotometer (Perkin Elmer Lambda-35, Wavelength 200 nm to 800 nm). The dispersion property of GO and Ag-GO nanoplates in water were measured using Zeta Sizer, Model Nano-ZS, Malvern Instruments Inc. (UK). Raman spectrophotometer equipped with a 532.23 nm wavelength laser source (WITec, Model: Alpha 300R) was used to confirm the formation of GO in this study.

2.3 Kirby-Bauer antibiotic testing

Kirby–Bauer antibiotic testing (KB testing or disc diffusion antibiotic sensitivity testing) was employed to test the silver-decorated GO's antimicrobial resistance. 20 µL of 1 mg·mL^{-1} GO and Ag-GO solution were dropped on 5 mm paper disk and left to dry overnight at room temperature. Escherichia coli K12 (*E. coli*), which were previously stored in glycerol solution at -4°C, were grown on Nutrient Agar at 35°C overnight. Afterwards, one colony of the grown bacteria was transferred to the nutrient broth and incubated for 8 h in order to reach 16×10^7 cells·mL^{-1} (OD 600 of 0.2). 20 µL of the solution was spread on a plate of nutrient agar. The paper disks containing GO and Ag-GO were placed and pressed on the center of each petri dish. After incubation at 35°C for 2 days, the growing colonies were observed through digital images of the plates, and the inhibition zone was measured [25].

3. Results and discussion

From the 10 g of graphite used for the synthesis of GO, about 0.6 g of under-oxidized material (residual graphite not converted to GO) was recorded for NGP while 2 g and 3.1 g were obtained for NGF and SGP, respectively. This showed that the yield of GO from NGP feedstock was much higher than the other two sources [5]. After the addition of sodium borohydride to the reaction solution consisting GO and $AgNO_3$, the color of synthesis solution changed from brown

to grey. This can be attributed to the restoration of silver nitrate by sodium borohydride and the formation of silver oxide on the surface of GO. This phenomenon has been reported by previous authors [26,27,30,32] and is an indication of a successful reaction between silver nitrate and sodium borohydride. Figure 1 shows the physical observation of NGP before and after the reaction. The color changed from brown to grey, which could be an indication of the deposition of Ag on the GO nanoplates owing to the existence of hydroxyl, epoxy, carbonyl, and carboxyl groups. After the reaction between silver nitrate and sodium borohydride that released the positive silver ions, these functional groups are used as anchors for the adsorption of silver and the formation of nanoparticles. Silver ions are preferably adsorbed on the basal planes and edges of GO. The oxygen elements in epoxy and hydroxyl groups of GO acted as the nucleation center for nanoparticles and stabilized them after growth. Based on this fact, a higher degree of oxidization of graphene oxide will result in more homogeneous nucleation and formation of silver nanoparticles on the GO nanoplates, which would be proven in subsequent analysis [33].

3.1 Raman analysis of silver decorated graphene oxide (Ag-GO)

Raman spectroscopy (Figure 2) indicated that all materials were quite similar. Raman spectra of all three materials showed a G band peak at around 1590 cm^{-1}, a primary in-plane vibrational mode, and a second-order overtone of a different in-plane vibration, D at around 1350 cm^{-1} peak from a 532 nm excitation laser. These peaks confirm the lattice distortion of GO and align well with the results shown by previous authors [34-36]. The higher number of functional groups of Ag-NGP can manifest itself in Raman spectra by the changes in the relative intensity of D and G peaks. Table 1 shows the Raman information and I_D/I_G ratio of all three samples. The D-band of the Ag-SGP, Ag-NGF and Ag-NGP is located at 1348.1 cm^{-1}, 1346.48 cm^{-1} and 1342.33 cm^{-1}, respectively. The D-band streams from a defect-induced breathing mode of sp^2 rings [37], and an increase of the D-peak intensity indicates the formation of more sp^2 domains. The relative intensity ratio of both peaks (I_D/I_G) is a measure of disorder degree and is inversely proportional to the average size of the sp^2 clusters [38,39]. These results suggest that more graphitic domains are present, and the sp^2 cluster number is higher for Ag-NGP when compared to NGF and SGP. The results indicate a greater number of silver decorated on the surface of Ag-NGP in comparison to Ag-SGP and Ag-NGF [40,41].

Figure 1. NGP before (left) and after (right) the decoration with silver.

3.2 X-ray diffraction (XRD) analysis

The XRD pattern for Ag-GO is shown in Figure 3. All the GO samples exhibit a carbon (001) diffraction peak at 2θ value in the range of 10° to 12°. The other peaks at about 38°, 44°, 64° and 77° are assigned to the Miller indices of (111), (200), (220), and (311) crystallographic planes of face-centred cubic (fcc) Ag nanoparticles, respectively. This result matched the data for the XRD standards exactly [42,43].

3.3 FESEM-EDX Analysis

Table 2 shows the EDX spectra information of the Ag-GO samples. The elemental composition of the samples showed the presence of silver (Ag), carbon (C), and oxygen (O). The ratio of oxygen to carbon for NGP sample is the highest among the three, and all the samples showed almost the same silver atomic ratio (around 2%). The higher ratio of oxygen is due to the existence of a higher number of functional groups, specifically epoxy and hydroxyl [44]. As mentioned before, these functional groups are the main active sites for the Ag nano-particles to anchor, nucleate, grow, and stabilize. As a result of the abundance of functional groups that provide more nucleation sites, mapping information of the samples indicated that the deposition of silver on NGP samples was more uniform than NGF and SGP, as shown in Figure 4-6.

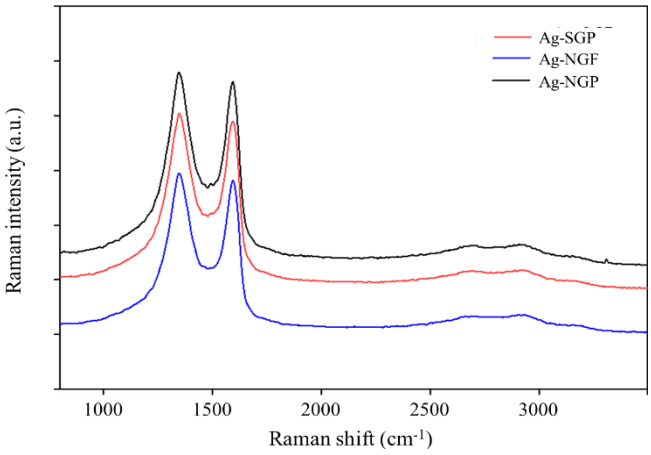

Figure 2. Raman shift of the produced silver decorated graphene oxide.

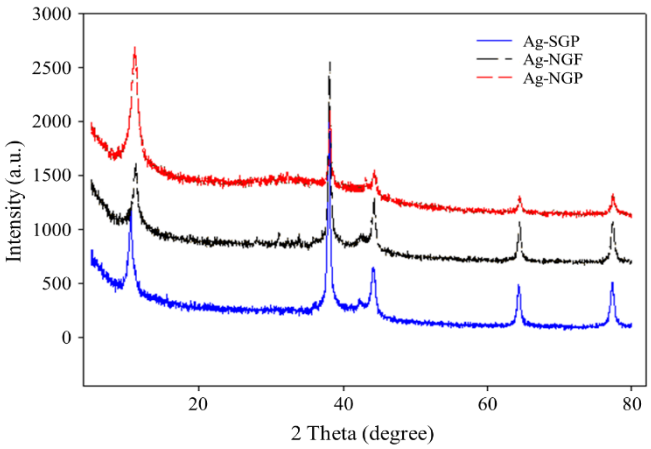

Figure 3. XRD patterns of produced silver decorated graphene oxide.

Table 1. Raman information of the produced silver decorated graphene oxide.

Sample name	D peak	G peak	I_D/I_G
Ag-SGP	1348.10	1593.20	1.01
Ag-NGF	1346.48	1591.64	1.02
Ag-NGP	1342.32	1591.64	1.09

Table 2. EDX results of produced silver decorated graphene oxide demonstrating the percentages of the elements.

Elements	Ag-NGP (wt%)	Ag-NGF (wt%)	Ag-SGP (wt%)	Ag-NGP (at%)	Ag-NGF (at%)	Ag-SGP (at%)
Carbon 0.277 keV	53.4	53.1	64.4	68.44	78.64	79.10
Oxygen 0.525 keV	30.4	27.4	20.4	29.25	18.70	18.83
Silver 2.984 keV	16.2	19.5	15.2	2.31	2.65	2.07

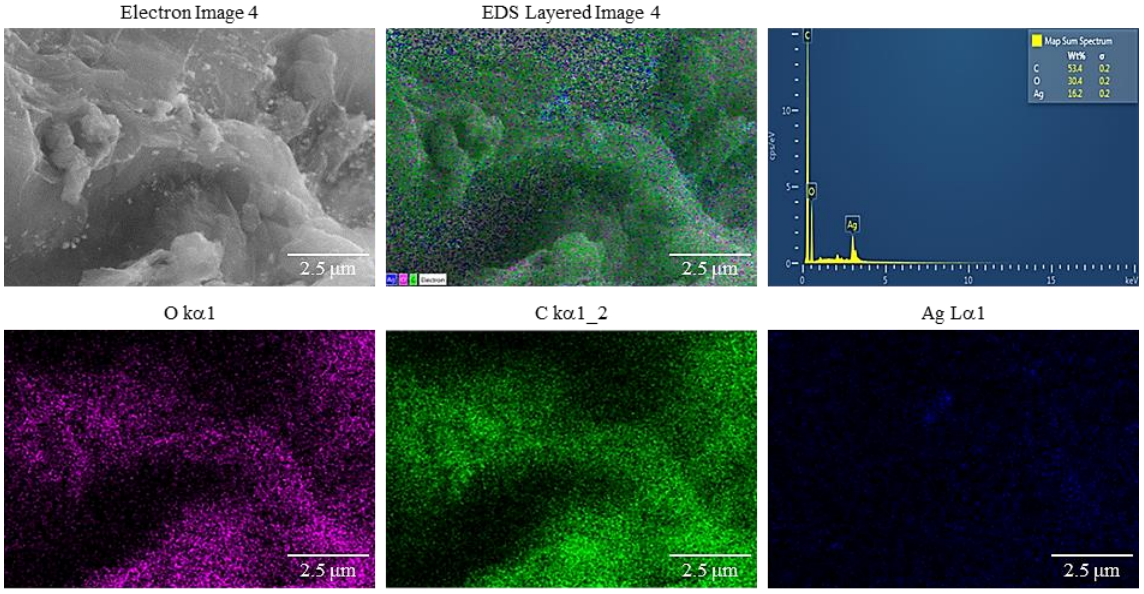

Figure 4. FESEM and EDX mapping results of Ag-NGP.

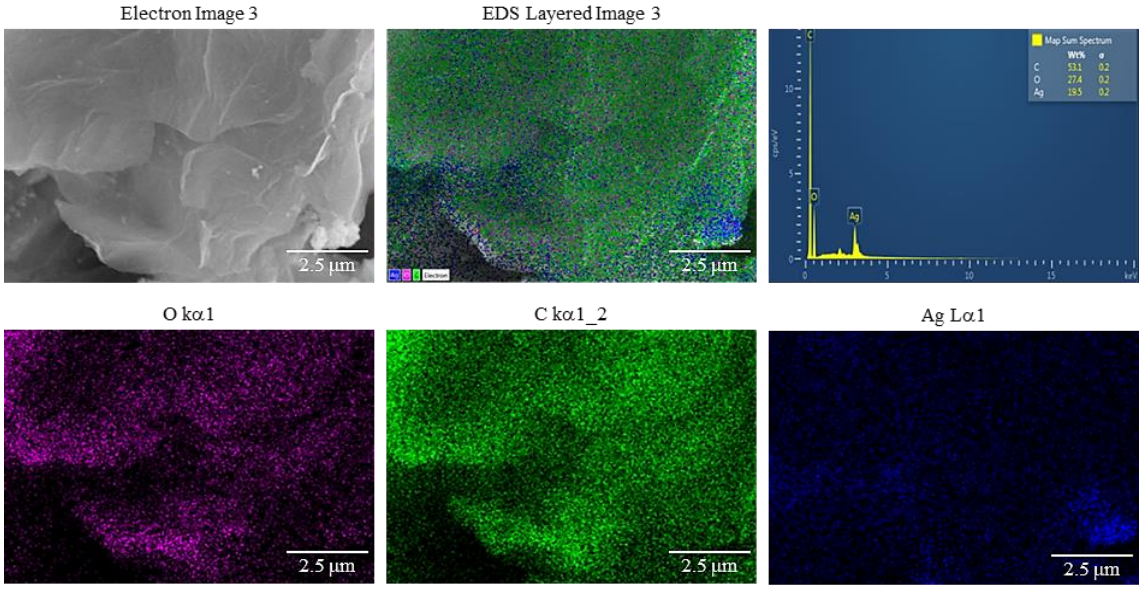

Figure 5. FESEM and EDX mapping results of Ag-NGF.

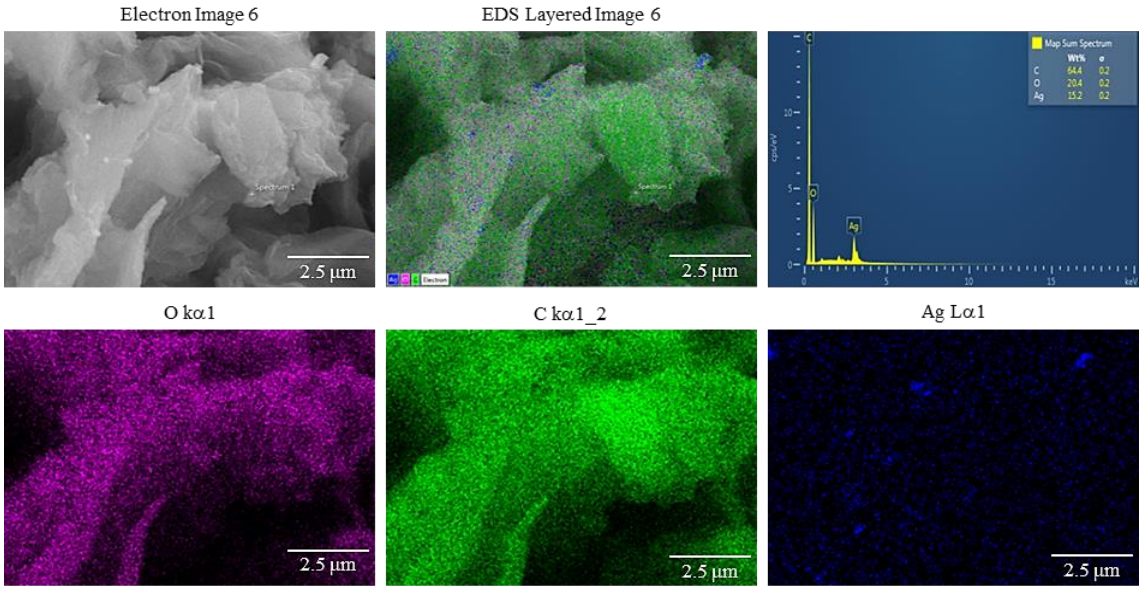

Figure 6. FESEM and EDX mapping results of Ag-SGP.

3.4 Transmission electron microscopy (TEM) analysis

In order to further probe the morphology and diffusion of the Ag on GO, TEM measurement was performed. An aqueous dispersion of Ag-GO was used for TEM scanning. This is also considered as a stability test for the Ag nanoparticles on the surface of the GO. The aqueous dispersion was prepared using sonication for 60 min. Sonication will remove the Ag nanoparticles from the surface of GO if the nucleation and bonding are not strong.

TEM results supported the results from EDX mapping of the material. Ag-NGP showed the smallest size of nanoparticles and uniform distribution along the surface of the nanoplates. This might be due to the higher degree of oxidization contributed by a higher number of the anchor points and better distribution of the silver ions. The TEM image (Figure 7) indicates that the average sizes of most of the silver nanoparticles were approximately 2 nm to 5 nm for NGP, 5 nm to 15 nm for NGF and 8 nm to 25 nm for SGP. A spherical geometry and a uniform distribution of the Ag across NGP sheet were observed. The sizes and uniform distributions of the nanoparticles are favorable to be used as the nanofiller that will be incorporated into the membrane structure. Smaller size means higher surface area and better distribution in the membrane matrix. This can prevent the agglomeration of silver nanoparticles in the membrane structure.

3.5 Zeta potential analysis

Zeta potential of the Ag-GO showed similar results to the GO. This suggests that the charge of all the nanomaterials is not affected by the decoration of Ag. The zeta potential of -47 mV is an assurance for the colloidal stability of the material, which is desirable for its dispersion in other application such as in membrane fabrication study. This phenomenon will help to decrease the chance of the aggregation of nanoparticles in membrane matrices during the fabrication phase.

3.6 UV-Vis Analysis

Plasmon band of Ag nanoparticles at 415 nm was observed, indicating the formation of bonding between Ag on GO nanoplates surface. The particular wavelength of the localized surface plasmon resonance depends on the Ag nanoparticle size, shape, and agglomeration state. As mentioned by previous authors, as the particle size increases, the absorbance peak increases from 400 nm to 500 nm and broadens in width [45]. Figure 8 shows that the UV-vis absorption of the obtained Ag-GO. All three samples show an absorption in violet and blue wavelengths range (400 nm to 500 nm), indicating the formation of Ag nanoparticles on the surface of GO. However, Ag-NGP sample showed a sharper peak around Violet wavelength, revealing that the

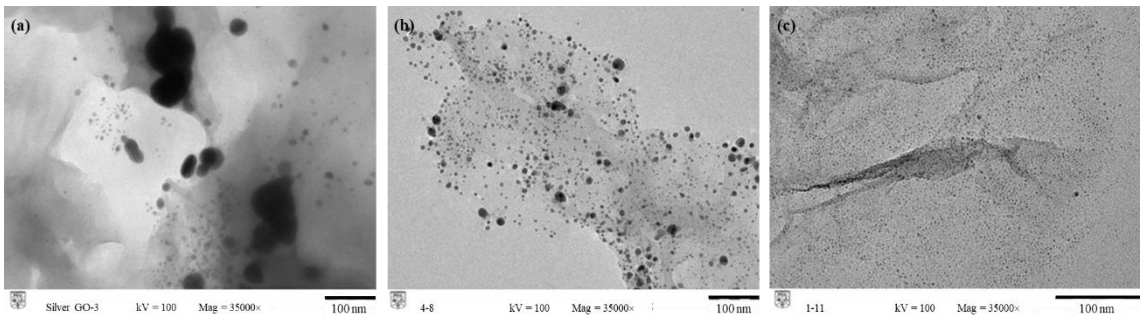

Figure 7. TEM results of produced silver decorated graphene oxide at 35000× magnifications: Ag-SGP (a), Ag-NGF (b), and Ag-NGP (c).

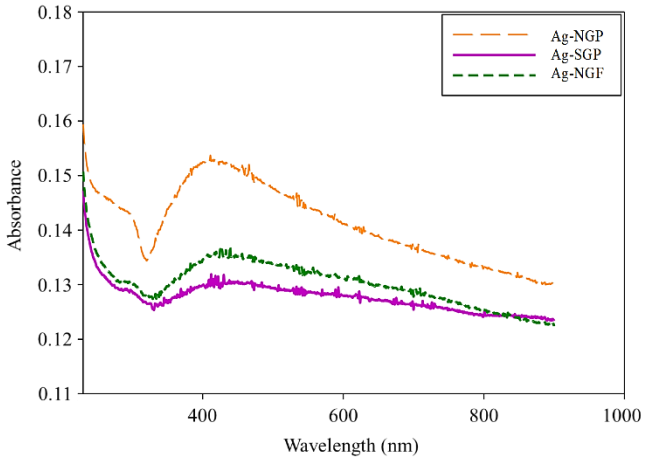

Figure 8. UV-Vis spectra of graphene oxide after decorated with Ag nanoparticles.

Ag nanoparticles formed on the surface of GO obtained from NGP were smaller in size [46]. The absorption of Ag-NGF and Ag-SGP was near the blue range (500 nm), indicating the formation of larger particles or agglomeration of nanoparticles on the surface of the GO. The result obtained by UV-vis supported the TEM and SEM results [10].

3.7 Kirby-Bauer antibiotic testing

Kirby–Bauer antibiotic testing was employed for Ag-GO samples. *E. coli* bacteria were used to compare the diameter of the inhibition zone (DIZ). In general, the DIZ has a direct relation to the effectiveness of the antibacterial material. The DIZ was measured using "Imagej" software for higher accuracy [47]. Figure 9 shows the DIZ of the graphene oxide decorated with silver. The results showed a significant DIZ due to the synergistic effects of graphene with a very low concentration of silver. Silver attacks the bacterial cells in two main ways: it makes the membrane cell more permeable, and it interferes with the cell's metabolism. This will lead to the overproduction of reactive and often toxic oxygen compounds [48-50]. Reports on the mechanism of antimicrobial properties of silver, also known as the oligodynamic effect, showed that immediately after coming into contact with the silver, microorganism DNA loses its replication ability [51]. Adenosine triphosphate (ATP) is an energy source used by intracellular organisms. Due to its role as energy storage, it plays a critical role in the bacteria's life [31]. Silver can affect the function of proteins and enzymes essential to ATP production. There are also other hypotheses, such as the silver nanoparticles could alter the bacteria membrane bonds and affect the Mitochondrial activities [25,50,52].

The antibacterial action of silver is dependent on the nanoparticle size and effective surface area. It can be observed in Figure 9 that the Ag-NGP DIZ diameter is 14.7 ± 1.2 mm. This is around 30% higher than those of Ag-NGF and Ag-SGF (10.25 ± 0.74 mm and 9.2 ± 0.52 mm, respectively). This could be due to smaller particle size and uniform particle distribution, which was previously observed in TEM and EDX-mapping of the Ag-NGP samples. This makes the NGP-Ag an ideal nanofiller for application such as membrane fabrication [1]. Similar antibacterial performance of silver nanoparticles-decorated GO has also been demonstrated in other studies, supporting the antibacterial property of the Ag-GO samples synthesized in this study [33,53,54].

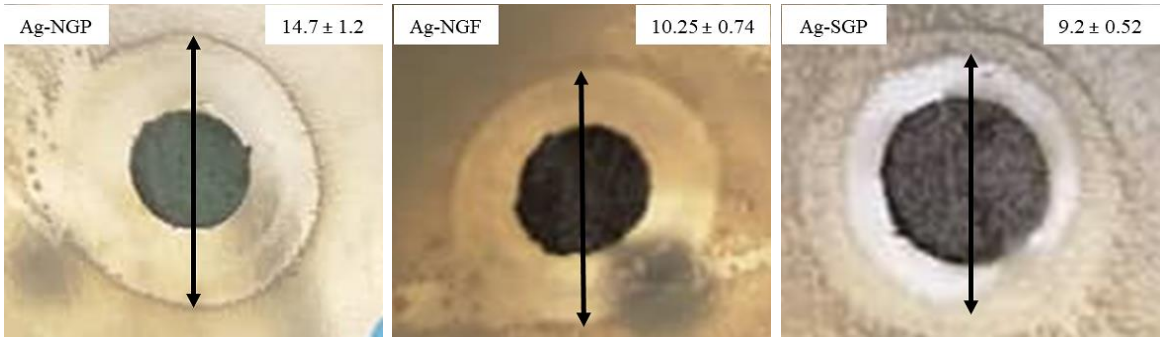

Figure 9. Kirby-Bauer antimicrobial results of Ag-GO.

4. Conclusions

Graphene oxide was successfully produced from different graphite sources. Graphite source selection proved to be a key factor in oxidization degree of the graphene oxide. Graphene oxide proved to be a great dispersion platform for silver nanoparticles. After the reaction, the silver decorated graphene oxide was analyzed and investigated using numerous tests. The findings indicated a successful decoration of silver on the surface of the graphene oxide. The formation of silver nanoparticles was confirmed by XRD analysis for all of the samples. EDX on mapping mode was employed to further study the formation of silver, which was in a good argument with XRD. TEM showed the average particles size of decorated silver NPs were approximately 2 nm to 5 nm for NGP, 5 nm to 15 nm for NGF and 8 to 25 for SGP. Additionally, Kirby–Bauer antibiotic testing revealed the diameter of the inhibition zone of NGP-Ag (14.7 ± 1.2 mm) was around 30% higher than those of NGF-Ag (10.25 ± 0.74 mm) and SGF-Ag (9.2 ± 0.52 mm). The consistency of the silver average particle size, spherical geometry, and a uniform distribution proved graphene oxide produced from NGP is an excellent dispersion platform.

Acknowledgements

The work was funded by the Special Program for Research Against COVID-19 (SPRAC), the ASEAN University Network/Southeast Asia Engineering Education Development Network (AUN/SEED-Net), Japan International Cooperation Agency (JICA).

References

[1] E. Mahmoudi, L. Y. Ng, W. L. Ang, Y. H. Teow, and A. W. Mohammad, "Improving membrane bioreactor performance through the synergistic effect of silver-decorated graphene oxide in composite membranes," *Journal of Water Process Engineering*, vol. 34, p. 101169, 2020.

[2] A. Nguyen, L. Zou, and C. Priest, "Evaluating the antifouling effects of silver nanoparticles regenerated by TiO_2 on forward osmosis membrane," *Journal of Membrane Science*, vol. 454, pp. 264-271, 2014.

[3] D. R. Dreyer, S. Park, C. W. Bielawski, and R. S. Ruoff, "The chemistry of graphene oxide," *Chemical Society Reviews*, vol. 39, pp. 228-240, 2010.

[4] A. Dufresne, "19 - Cellulose-based composites and nanocomposites," in *Monomers, Polymers and Composites from Renewable Resources*, ed Elsevier, 2008, pp. 401-418.

[5] E. Mahmoudi, W. L. Ang, C. Y. Ng, L. Y. Ng, A. W. Mohammad, and A. Benamor, "Distinguishing characteristics and usability of graphene oxide based on different sources of graphite feedstock," *Journal of Colloid and Interface Science*, vol. 542, pp. 429-440, 2019.

[6] D. R. Dreyer, R. S. Ruoff, and C. W. Bielawski, "From conception to realization: An historial account of graphene and some perspectives for its future," *Angewandte Chemie - International Edition*, vol. 49, pp. 9336-9344, 2010.

[7] D. C. Marcano, D. V. Kosynkin, J. M. Berlin, A. Sinitskii, Z. Sun, A. Slesarev, L. B. Alemany, W. Lu, and J. M. Tour, "Improved synthesis of graphene oxide," *ACS Nano*, vol. 4, pp. 4806-4814, 2010.

[8] C. N. R. Rao, K. S. Subrahmanyam, H. S. S. R. Matte, and A. Govindaraj, "Graphene: Synthesis, functionalization and properties," *Modern Physics Letters B*, vol. 25, pp. 427-451, 2011.

[9] V. Georgakilas, M. Otyepka, A. B. Bourlinos, V. Chandra, N. Kim, K. C. Kemp, P. Hobza, R. Zboril, and K. S. Kim, "Functionalization of graphene: Covalent and non-covalent approaches, derivatives and applications," *Chemical Reviews*, vol. 112, pp. 6156-6214, 2012.

[10] S. Pipattanachat, J. Qin, D. Rokaya, P. Thanyasrisung, and V. Srimaneepong, "Biofilm inhibition and bactericidal activity of NiTi alloy coated with graphene oxide/silver nanoparticles via electrophoretic deposition," *Scientific Reports*, vol. 11, pp. 1-9, 2021.

[11] D. Rokaya, V. Srimaneepong, J. Qin, P. Thunyakitpisal, and K. Siraleartmukul, "Surface adhesion properties and cytotoxicity of graphene oxide coatings and graphene oxide/silver nanocomposite coatings on biomedical NiTi alloy," *Science of Advance Material*, vol. 11, pp. 1474-1487, 2019.

[12] J. Jin, R. Rafiq, Y. Q. Gill, and M. Song, "Preparation and characterization of high performance of graphene/nylon nanocomposites," *European Polymer Journal*, vol. 49, pp. 2617-2626, 2013.

[13] C. Zhao, X. Xu, J. Chen, G. Wang, and F. Yang, "Highly effective antifouling performance of PVDF/graphene oxide composite membrane in membrane bioreactor (MBR) system," *Desalination*, vol. 340, pp. 59-66, 2014.

[14] X. R. Li, J. J. Xu, and H. Y. Chen, "12 - Chemical modification of graphene," in *Graphene Science Handbook*, ed Routledge: CRC Press, 2016, pp. 207-223.

[15] H. Ahmad, M. Fan, and D. Hui, "Graphene oxide incorporated functional materials: A review," *Composites Part B: Engineering*, vol. 145, pp. 270-280, 2018.

[16] M. A. Ashraf, W. Peng, Y. Zare, and K. Y. Rhee, "Effects of size and aggregation/agglomeration of nanoparticles on the interfacial/interphase properties and tensile strength of polymer nanocomposites," *Nanoscale Research Letters*, vol. 13, p. 214, 2018.

[17] L. Jiang, J. Yun, Y. Wang, H. Yang, Z. Xu, and Z. L. Xu, "High-flux, anti-fouling dendrimer grafted PAN membrane: Fabrication, performance and mechanisms," *Journal of Membrane Science*, vol. 596, p. 117743, 2020.

[18] M. Golpour, and M. Pakizeh, "Preparation and characterization of new PA-MOF/PPSU-GO membrane for the separation of KHI from water," *Chemical Engineering Journal*, vol. 345, pp. 221-232, 2018.

[19] Q. Bao, D. Zhang, and P. Qi, "Synthesis and characterization of silver nanoparticle and graphene oxide nanosheet composites as a bactericidal agent for water disinfection," *Journal of Colloid and Interface Science*, vol. 360, pp. 463-470, 2011.

[20] S. Kim, B. Tserengombo, S. H. Choi, J. Noh, S. Huh, B. Choi, H. Chung, J. Kim, and H. Jeong, "Experimental investigation of dispersion characteristics and thermal conductivity of various surfactants on carbon based nanomaterial," *International Communications in Heat and Mass Transfer*, vol. 91, pp. 95-102, 2018.

[21] W. Kiciński, and S. Dyjak, "Transition metal impurities in carbon-based materials: Pitfalls, artifacts and deleterious effects," *Carbon*, vol. 168, pp. 748-845, 2020.

[22] B. F. Abu-Sharkh, and H. Hamid, "Degradation study of date palm fibre/polypropylene composites in natural and artificial weathering: mechanical and thermal analysis," *Polymer Degradation and Stability*, vol. 85, pp. 967-973, 2004.

[23] L. Y. Ng, A. W. Mohammad, C. P. Leo, and N. Hilal, "Polymeric membranes incorporated with metal/metal oxide nanoparticles: A comprehensive review," *Desalination*, vol. 308, pp. 15-33, 2013.

[24] J. Yang, C. Zang, L. Sun, N. Zhao, and X. Cheng, "Synthesis of graphene/Ag nanocomposite with good dispersibility and electroconductivity via solvothermal method," *Materials Chemistry and Physics*, vol. 129, pp. 270-274, 2011.

[25] Q. Bao, D. Zhang, and P. Qi, "Synthesis and characterization of silver nanoparticle and graphene oxide nanosheet composites as a bactericidal agent for water disinfection," *Journal of Colloid Interface Science*, vol. 360, pp. 463-470, 2011.

[26] S. V. Kumar, N. M. Huang, H. N. Lim, A. R. Marlinda, I. Harrison, and C. H. Chia, "One-step size-controlled synthesis of functional graphene oxide/silver nanocomposites at room temperature," *Chemical Engineering Journal*, vol. 219, pp. 217-224, 2013.

[27] M. R. Das, R. K. Sarma, R. Saikia, V. S. Kale, M. V. Shelke, and P. Sengupta, "Synthesis of silver nanoparticles in an aqueous suspension of graphene oxide sheets and its antimicrobial activity," *Colloids and Surfaces B: Biointerfaces*, vol. 83, pp. 16-22, 2011.

[28] B. Yang, Z. Liu, Z. Guo, W. Zhang, M. Wan, X. Qin, and H. Zhong, "In situ green synthesis of silver–graphene oxide

nanocomposites by using tryptophan as a reducing and stabilizing agent and their application in SERS," *Applied Surface Science*, vol. 316, pp. 22-27, 2014.

[29] G. Moon, H. Kim, Y. Shin, and W. Choi, "Chemical-free growth of metal nanoparticles on graphene oxide sheets under visible light irradiation," *RSC Advances*, vol. 2, pp. 2205-2207, 2012.

[30] V. G. Watson, *Decoration of graphene oxide with silver nanoparticles and controlling the silver nanoparticle loading on graphene*. University of Dayton, 2014.

[31] I. M. Daniel, and O. Ishai, *Engineering mechanics of composite materials*. New York: Oxford University Press, 2006.

[32] J. Ma, J. Zhang, Z. Xiong, and Y. Yong, "Preparation, characterization and antibacterial properties of silver-modified graphene oxide," *Journal of Materials Chemistry*, vol. 21, pp. 3350-3352, 2011.

[33] N. T. Huong, N. M. Dat, D. B. Thinh, T. N. Minh Anh, D. M. Nguyet, T. H. Quan, P. N. Bao Long, H. M. Nam, M. T. Phong, and N. H. Hieu, "Optimization of the antibacterial activity of silver nanoparticles-decorated graphene oxide nanocomposites," *Synthetic Metals*, vol. 268, p. 116492, 2020.

[34] Y. Xie, Y. Li, L. Niu, H. Wang, H. Qian, and W. Yao, "A novel surface-enhanced Raman scattering sensor to detect prohibited colorants in food by graphene/silver nanocomposite," *Talanta*, vol. 100, pp. 32-37, 2012.

[35] A. N. Sidorov, G. W. Sławiński, A. H. Jayatissa, F. P. Zamborini, and G. U. Sumanasekera, "A surface-enhanced Raman spectroscopy study of thin graphene sheets functionalized with gold and silver nanostructures by seed-mediated growth," *Carbon*, vol. 50, pp. 699-705, 2012.

[36] W. X. Wang, S. H. Liang, T. Yu, D. H. Li, Y. B. Li, and X. F. Han, "The study of interaction between graphene and metals by Raman spectroscopy," *Journal of Applied Physics*, vol. 109, p. 07C501, 2010.

[37] G. Sobon, J. Sotor, J. Jagiello, R. Kozinski, M. Zdrojek, M. Holdynski, P. Paletko, J. Boguslawski, L. Lipinska, and K. M. Abramski, "Graphene oxide vs reduced graphene oxide as saturable absorbers for er-doped passively mode-locked fiber laser," *Optics Express*, vol. 20, pp. 19463-19473, 2012.

[38] L. Tao, Y. Lou, Y. Zhao, M. Hao, Y. Yang, Y. Xiao, Y. H. Tsang, and J. Li, "Silver nanoparticle-decorated graphene oxide for surface-enhanced Raman scattering detection and optical limiting applications," *Journal of Materials Science*, vol. 53, pp. 573-580, 2018.

[39] X. Zhou, X. Huang, X. Qi, S. Wu, C. Xue, F. Y. C. Boey, Q. Yan, P. Chen, and H. Zhang, "In situ synthesis of metal nanoparticles on single-layer graphene oxide and reduced graphene oxide surfaces," *The Journal of Physical Chemistry C*, vol. 113, pp. 10842-10846, 2009.

[40] L. Hu, Y. J. Liu, Y. Han, P. Chen, C. Zhang, C. Li, Z. Lu, D. Luo, and S. Jiang, "Graphene oxide-decorated silver dendrites for high-performance surface-enhanced Raman scattering applications," *Journal of Materials Chemistry C*, vol. 5, pp. 3908-3915, 2017.

[41] J. Prakash Singh, T. Nandi, and S. Kumar Ghosh, "Structure-property relationship of silver decorated functionalized reduced graphene oxide based nanofluids: Optical and thermophysical aspects and applications," *Applied Surface Science*, vol. 542, p. 148410, 2021.

[42] S. Li, Y. Shen, A. Xie, X. Yu, L. Qiu, L. Zhang, and Q. Zhang, "Green synthesis of silver nanoparticles using Capsicum annuum L. extract," *Green Chemistry*, vol. 9, pp. 852-858, 2007.

[43] M. Cobos, I. De-La-Pinta, G. Quindós, M. J. Fernández, and M. D. Fernández, "Graphene oxide–silver nanoparticle nanohybrids: Synthesis, characterization, and antimicrobial properties," *Nanomaterials*, vol. 10, p. 376, 2020.

[44] Y. Li, M. Liao, and J. Zhou, "Catechol and its derivatives adhesion on graphene: Insights from molecular dynamics simulations," *The Journal of Physical Chemistry C*, vol. 122, pp. 22965-22974, 2018.

[45] J. Lu, J. J. Bravo-Suárez, A. Takahashi, M. Haruta, and S. T. Oyama, "In situ UV–vis studies of the effect of particle size on the epoxidation of ethylene and propylene on supported silver catalysts with molecular oxygen," *Journal of Catalysis*, vol. 232, pp. 85-95, 2005.

[46] W. Haiss, N. T. K. Thanh, J. Aveyard, and D. G. Fernig, "Determination of size and concentration of gold nanoparticles from UV−Vis spectra," *Analytical Chemistry*, vol. 79, pp. 4215-4221, 2007.

[47] A. Salleh, R. Naomi, N. D. Utami, A. W. Mohammad, E. Mahmoudi, N. Mustafa, and M. B. Fauzi, "The potential of silver nanoparticles for antiviral and antibacterial applications: A mechanism of action," *Nanomaterials*, vol. 10, pp. 1-20, 2020.

[48] Y. Jiang, J. L. Gong, G. M. Zeng, X. M. Ou, Y. N. Chang, C. H. Deng, J. Zhang, H. Y. Liu, and S. Y. Huang, "Magnetic chitosan-graphene oxide composite for anti-microbial and dye removal applications," *International Journal of Biological Macromolecules*, vol. 82, pp. 702-710, 2016.

[49] S. Kar, B. Bagchi, B. Kundu, S. Bhandary, R. Basu, P. Nandy, and S. Das, "Synthesis and characterization of Cu/Ag nanoparticle loaded mullite nanocomposite system: A potential candidate for antimicrobial and therapeutic applications," *Biochimica et Biophysica Acta (BBA) - General Subjects*, vol. 1840, pp. 3264-3276, 2014.

[50] I. Sondi, and B. Salopek-Sondi, "Silver nanoparticles as antimicrobial agent: a case study on *E. coli* as a model for Gram-negative bacteria," *Journal of Colloid and Interface Science*, vol. 275, pp. 177-182, 2004.

[51] H. Park, J. Y. Kim, J. Kim, J. Lee, J.-S. Hahn, M. B. Gu, and J. Yoon, "Silver-ion-mediated reactive oxygen species generation affecting bactericidal activity," *Water Research*, vol. 43, pp. 1027-1032, 2009.

[52] X.-F. Sun, J. Qin, P.-F. Xia, B.-B. Guo, C.-M. Yang, C. Song, and S.-G. Wang, "Graphene oxide–silver nanoparticle membrane for biofouling control and water purification," *Chemical Engineering Journal*, vol. 281, pp. 53-59, 2015.

[53] A. K. Potbhare, M. S. Umekar, P. B. Chouke, M. B. Bagade, S. K. Tarik Aziz, A. A. Abdala, and R.G. Chaudhary, "Bioinspired graphene-based silver nanoparticles: Fabrication, characterization and antibacterial activity," *Materials Today Proceeding*, vol. 29, pp. 720-725, 2020.

[54] L. Ma, Z. Zhu, M. Su, L. Ma, D. Liu, and Z. Wang, "Preparation of graphene oxide–silver nanoparticle nanohybrids with highly antibacterial capability," *Talanta*, vol. 117, pp. 449-455, 2013.